研究成果の刊行に関する一覧表

発表者氏名	論文タイトル名	発表誌名　巻号：ページ	出版年
遠藤登喜子	マンモグラフィ検診精度管理中央委員会について	Rad Fan 2(4)：28-31	2004
遠藤登喜子	マンモグラフィ	臨床婦人科産科　58(7)：884-887	2004
遠藤登喜子	わが国の乳がん検診ー現状と最近の動きー	日本医学放射線学会誌 64(5)：277-283	2004
遠藤登喜子	画像診断でどこまでわかるか　ー乳房良性・悪性病変のマンモグラフィ診断法ー	産婦人科の実際　53(8)：1143-1150	2004
遠藤登喜子	総合的画像診断の進め方	乳癌の臨床　19(4)：313-321	2004
遠藤登喜子	乳腺疾患　マンモグラフィでここまで読める	Medicina 41(12)：194-202	2004
栗山浩一、遠藤登喜子、他	乳房X線写真上の腫瘤陰影検出システムにおける類似画像検索法を用いた偽陽性削除法	電子情報通信学会論文誌 D-II J87-D-II(1)：353-356	2004
遠藤登喜子	乳がん早期発見の画像診断(1)　マンモグラフィ検診を中心に	明日の臨床　16(2)：1-6	2004
藤田広志、遠藤登喜子、他	乳腺超音波画像におけるCAD	映像情報MEDICAL 36(4)：410-414	2004
遠藤登喜子、他	新春座談会　スーパーテクノロジストを語る	日本放射線技術学会雑誌 60(1)：1-18	2004
Kakinuma R., Tsuchiya R., Eguchi K., Kaneko M., et al.	Progression of focal pure ground-glass opacity detected by low-dose helical computed tomography screening for lung cancer.	J Comput Assist Tomogr 28(1)：17-23	2004
柿沼龍太郎、金子昌弘、他	肺癌CT検診での結節の診断基準	臨床放射線　49(3)：369-376	2004
金子昌弘、柿沼龍太郎、土屋了介、他	肺癌検診の意義	内科　95(1)：20-23	2005
金子昌弘、土屋了介、他	わが国におけるCT肺癌検診　変遷と現状	臨床放射線　49：353-359	2004
金子昌弘、柿沼龍太郎、他	肺がん検診におけるFDG-PETの役割	臨床放射線　49：873-879	2004
金子昌弘、他	低線量CTによる肺がん検診の有用性に関する研究	胸部CT検診　11(2)：87-90	2004
松井英介、金子昌弘、他	顕微鏡CTによる末梢気道・肺病変の形態解析	胸部CT検診　11(2)：129-135	2004
中園智昭、金子昌弘、他	胸部CT検診読影の実際（幕張にて肺がんをなくす会）	胸部CT検診　11(3)：209-211	2004

研究成果の刊行に関する一覧表

発表者氏名	論文タイトル名	発表誌名 巻号: ページ	出版年
楠本昌彦、 金子昌弘、 他	これだけでわかる画像による悪性腫瘍の病期診断　肺	臨床画像 20(11) : 30-41	2004
楠本昌彦、 金子昌弘、 他	小型肺結節のＣＴ診断	呼吸器科 6(3): 214-222	2004
Yatabe Y., Mitsudomi T., et al.	CK20 expression, CDX2 expression, K-ras mutation, and goblet cell morphology in a subset of lung adenocarcinomas.	J Pathol 203: 645-652	2004
Yatabe Y., Mitsudomi T., et al.	Maspin expression in normal lung and non-small-cell lung cancers: cellular property-associated expression under the control of promoter DNA methylation.	Oncogene 23: 4041-4049	2004
Tomida S., Mitsudomi T., et al.	Gene expression-based, individualized outcome prediction for surgically treated lung cancer patients.	Oncogene 23: 1-11	2004
Takamizawa J., Mitsudomi T., et al.	Reduced expression of the let-7 microRNAs in human lung cancers in association with shortened postoperative survival.	Cancer Res 64: 3753-3756	2004
Tajima K., Mitsudomi T., et al.	Identification of an epitope from the epithelial cell adhesion molecule eliciting HLA-A*2402-restricted cytotoxic T lymphocyte responses.	Tissue Antigens 64: 650-659	2004
Tajima K., Mitsudomi T., et al.	Interferon-gamma differentially regulates susceptibility of lung cancer cells to telomerase-specific cytotoxic T lymphocytes.	Int J Cancer 110: 403-412	2004
Suzuki T., Mitsudomi T., et al.	The impact of EGFR mutations on gefitinib sensitivity in non-small cell lung cancer.	Personalized Med 1(1): 27-34	2004
Osada H., Mitsudomi T., et al.	Reduced expression of class II histone deacetylase genes is associated with poor prognosis in lung cancer patients.	Int J Cancer 112: 26-32	2004
Kosaka T., Mitsudomi, T., et al.	Mutations of the epidermal erowth eactor eeceptor gene in lung cancer: Biological and clinical implications.	Cancer Res 64: 8919-8923	2004

研究成果の刊行に関する一覧表

発表者氏名	論文タイトル名	発表誌名　巻号：ページ	出版年
Koga T., Mitsudomi T., et al.	Identification of MGB1 as a marker in the differential diagnosis of lung tumors in patients with a history of breast cancer by analysis of publicly available SAGE data.	J Mol Diagn 6(2)：90-95	2004
Ito H., Mitsudomi T., et al.	Gene-environment interactions between the smoking habit and polymorphisms in the DNA repair genes, APE1 Asp148Glu and XRCC1 Arg399Gln, in Japanese lung cancer risk.	Carcinogenesis 25(8)：1395-1401	2004
Endoh H., Mitsudomi T., et al.	Prognostic model of pulmonary adenocarcinoma by expression profiling of eight genes as determined by quantitative real-time reverse transcriptase polymerase chain reaction.	J Clin Oncol 22(5)：811-819	2004
Marugame T., Hamashima C.	Mortality trend of uterine cancer in Japan:1960-2000.	Jpn J Clin Oncol　34(1)：55-56	2004
村山正博、濱島ちさと、他	2004日本臨床スポーツ医学会学術委員会公開シンポジウム　スポーツと医療経済：運動習慣は医療費を削減できるか	臨床スポーツ医学　21(7)：774-802	2004
濱島ちさと	がん検診の有効性	からだの科学　238：46-49	2004
濱島ちさと	海外における経済評価ガイドライン	臨床研究・生物統計研誌 24(1)：13-18	2004
濱島ちさと	がん検診の有効性評価	公衆衛生　68(12):977-980	2004
濱島ちさと	総特集予防医学はどこまで可能か 米国予防サービス委員会に見る大腸がん検診の経済評価	新医療　2月号：72-74	2005
Okamura T., Okayama A., et al.	Resting heart rate cause-specific death in a 16.5-year cohort study of the Japanese general population.	American Heart Journal 147(6)：1024-1032	2004
Ueshima H., Okayama A., et al.	Cigarette smoking as arisk factor for stroke death in Japan Nippon Data80.	Storoke 35：1836-1841	2004
＜平成15年度＞			
Hotta K., Tsuchiya R.	Distant failure after treatment of postoperative locoregional recurrence of non-small cell lung cancer.	Thoracic Cardiov Surg 51：283-287	2003
Ikeda N., et al.	Histopathological evalution of fluorescence bronchoscopy using resected lungs in cases of lung cancer.	Lung cancer 41：303-309	2003

研究成果の刊行に関する一覧表

発表者氏名	論文タイトル名	発表誌名　巻号：ページ	出版年
Ikeda N., et al.	A clinicopathological study of resected adenocarcinoma 2 cm or less in diameter.	Ann Thorac Surg 78: 1011-1016	2004
池田徳彦、他	特集　肺癌　中心型早期肺癌の診断と治療	病理と臨床　21(5)：481-486	2003
池田徳彦、他	特集　肺癌：診断・治療の最前線　内視鏡的蛍光診断	癌の臨床　49(10)：1071-1076	2003
池田徳彦、他	総説　肺癌の内視鏡診断　-最近の進歩を中心に-	呼吸　22(10)：939-944	2003
池田徳彦、他	ガイドラインからみた肺癌外科の構築　4.リンパ節転移を伴う肺癌の治療ガイドライン	日本外科学会雑誌 105(7)：404-407	2004
遠藤登喜子、他	マンモグラフィを読む！カテゴリー分類の完全マスター	画像診断　23(10)：1206-1215	2003
遠藤登喜子、他	特集　ITと画像診断の進歩　CADによる乳癌診断	日獨医報　48(1)：30-38	2003
遠藤登喜子	教育講座　-知っておくと役立つ画像診断シリーズ-＜乳房領域＞　乳房撮影	日本放射線技術学会雑誌 59(6)：700-706	2003
杜下淳次、遠藤登喜子、他	第59回総会学術大会シンポジウムIII　コンピュータ支援診断：魅力と課題	日本放射線技術学会雑誌 59(11)：1338-1360	2003
遠藤登喜子	乳癌の現状とマンモグラフィ検診 -本当に役立つ検診の条件-		2003
Endoh H., Mitsudomi T., et al.	Rassfia gene inactivation in non-small cell lung cancer and its clinical implication.	Int J Cancer 106: 45-51	2003
Hanai T., Mitsudomi T., et al.	Prognostic models in patiens with non-small-cell lung cancer using artificial neural networks in comparison with logstic regression.	Cancer Sci 94(5)：473-477	2003

書籍

著者氏名	論文タイトル名	書籍全体の編集者名	書籍名	出版社名	出版地	出版年	ページ
＜平成17年度＞							
Endo T., et al.	Draft diagnostic guidelines for non-mass image forming lesions by the Japan Association of Breast and Thyrod Sonology(JABTS) and the Japan Society of Ultrasonics in Medicine.	Ueno E., Shiina T., Kubota M., Sawai K.	Research and Development in Breast Ultrasound	Springer	Japan	2005	89-100

研究成果の刊行に関する一覧表

著者氏名	論文タイトル名	書籍全体の編集者名	書籍名	出版社名	出版地	出版年	ページ
柿沼龍太郎、江口研二、金子昌弘、土屋了介	Ⅲ. 診断の進歩　10. 低線量CTによる肺癌検診のガイドライン	工藤翔二、土屋了介、金沢実、大田健	Annual Review　呼吸器 2006	中外医学社	東京	2006	185-192
濱島ちさと	第6章　予防医学領域における分析事例	池上直己、西村周三	医療技術・医薬品	勁草書房	東京	2005	141-162
＜平成16年度＞							
江口研二	18. 胸部Ｘ線写真・胸部ＣＴ検査異常とその対応	小川哲平、猿田亮男、田村政紀	健診・人間ドックハンドブック	中外医学社	東京	2004	175-181
江口研二	低線量ＣＴによる肺癌検診の手引き	低線量ＣＴによる肺癌検診のあり方に関する合同委員会	低線量ＣＴによる肺癌検診の手引き	金原出版	東京	2004	iii-v
金子昌弘	本邦におけるＣＴ検診の歴史とその広がり	低線量ＣＴによる肺癌検診のあり方に関する合同委員会	低線量ＣＴによる肺癌検診の手引き	金原出版	東京	2004	19-21
金子昌弘	ヘリカルCT	三木一正、渡邊能行	がん検診計画ハンドブック	南江堂	東京	2004	56-59
金子昌弘	2. 末梢小型肺癌の発見法	加藤治文、小林紘一、近藤　丘、清水信義、白日高歩、和田洋巳	最先端シリーズ２６　呼吸器外科：呼吸器外科の最新医療	先端医療技術研究所	東京	2004	136-141
村松幸男	X線診断の基礎と要点	松江寛人、廣田映五	乳腺画像診断法　X線．超音波と病理	金原出版	東京	2004	26-31, 52-243
光冨徹哉、他	分子マーカー　EGFR遺伝子変異の発見の衝撃	加藤治文、西條長宏、福岡正博、小林紘一、海老原善郎、井内康輝、早川和重	MOOK 肺癌の臨床 2004-2005	篠原出版新社	東京	2005	247-257
濱島ちさと、他	スクリーニングとその適用	田中平三、辻一郎、吉池信男、大賀英史、他	健康・栄養科学シリーズ社会・環境と健康	南江堂	東京	2004	94-97
濱島ちさと	経済評価からみたがん検診	三木一正、渡邊能行	住民検診・職域検診・人間ドックのためのがん検診計画ハンドブック	南江堂	東京	2004	14-18

研究成果の刊行に関する一覧表

著者氏名	論文タイトル名	書籍全体の編集者名	書籍名	出版社名	出版地	出版年	ページ
濱島ちさと、他	悪性新生物の第２次予防対策	大野良之、他	生活習慣病予防マニュアル第４版	南山堂	東京	2004	142-154

Radiologic Classification of Small Adenocarcinoma of the Lung: Radiologic-Pathologic Correlation and Its Prognostic Impact

Kenji Suzuki, MD, Masahiko Kusumoto, MD, Shun-ichi Watanabe, MD, Ryosuke Tsuchiya, MD, and Hisao Asamura, MD

Thoracic Surgery Division and Diagnostic Radiology, National Cancer Center Hospital, Tokyo, Japan

Background. A new radiologic classification for small adenocarcinoma is necessary for discussions of limited surgical resection for peripheral lung cancer.

Methods. Between 1999 and 2003, 1,697 consecutive patients underwent pulmonary resection for lung cancer. Three hundred forty-nine of these patients with clinical stage IA lung cancer who had lung peripheral adenocarcinoma, 2 cm or less in size, were investigated retrospectively. Radiologic classification was based on the findings of thin-section computed tomographic scan such as the presence of solid and ground-glass opacity (GGO). Type 1 (n = 22), type 2 (n = 26), type 3 (n = 25), and type 4 (n = 43) show a simple GGO, an intermediate homogeneous increase in density, a halo, and a mixed area of GGO and a solid, respectively. Type 5 (n = 54) shows a solid tumor with GGO, and type 6 (n = 179) shows a solid tumor.

Results. There was no difference in the maximum tumor dimension among the six groups. All but 1 patient had no lymph node metastases among type 1 to 4 tumors, whereas these were found in 5% and 24% of the patients with type 5 and 6 tumors, respectively. Lymphatic invasions were rarely found in patients with type 1 to 4 tumors ($p < 0.001$).

Conclusions. Types 1, 2, 3, and 4 are considered to be radiologic early adenocarcinoma of the lung, and their pathologic features were minimally invasive. On the other hand, type 5 and 6 tumors could have lymph node metastases and are considered to be invasive adenocarcinoma. Although limited surgical resection may be enough for type 1 to 4 tumors, anatomic pulmonary resection should be recommended for type 5 or 6 tumor.

(Ann Thorac Surg 2006;81:413–20)

Several authors have reported that the incidence of adenocarcinoma of the lung has been increasing [1, 2]. The introduction of computed tomography (CT) for screening of lung cancer has made it possible to detect smaller pulmonary nodules. Most of those pulmonary nodules are peripherally located adenocarcinoma of the lung, and such early detection may be associated with attainment of cure through early intervention [3, 4]. Although there is a general consensus regarding the pathologic diagnosis of early adenocarcinoma of the lung [5–8], the clinical and radiologic diagnosis of early adenocarcinoma with favorable prognosis is still controversial. Several authors have reported that adenocarcinoma of the lung that shows a wide area of ground-glass opacity (GGO) has a good prognosis [4, 9–15]. However, there is no generally accepted method for measuring the area of GGO, as it is sometimes difficult to divide peripherally located adenocarcinomas according to the existing classification. Thus, a new classification of peripherally located adenocarcinoma of the lung is necessary, and in this study we sought to determine how to best classify peripherally located adenocarcinoma of the lung retrospectively.

Patients and Methods

Patient Characteristics

Between January 1999 and December 2003, 1,697 consecutive patients underwent pulmonary resection for lung cancer. Among them, 349 patients with clinical stage IA lung cancer who had peripherally located adenocarcinoma of the lung 2 cm or less in size were investigated in this study. Patients who received preoperative treatment, such as radiotherapy or chemotherapy, or who had multiple lung cancers were excluded from the study. Informed consent was obtained from the patients. Of these, 167 were men and 182 were women. Their ages ranged from 23 to 89 years, with a median of 64 years.

Radiologic Evaluation

Contrast-enhanced CT scan was performed using a TCT 900S or X-Vigor (Toshiba, Tokyo, Japan), and 10-mm-thick contiguous collimation was used to evaluate the entire lung for preoperative staging. The size of tumors was determined digitally based on the findings of thin-section CT

Accepted for publication July 18, 2005.

Address correspondence to Dr Suzuki, Thoracic Surgery Division, National Cancer Center Hospital, 1-1, Tsukiji 5-chome, Chuo-ku, Tokyo 104-0045, Japan; e-mail: kjsuzuki@ncc.go.jp.

0003-4975/06/$32.00
doi:10.1016/j.athoracsur.2005.07.058

Table 1. Radiologic Classification of Small Adenocarcinoma of Lung by Means of Thoracic Thin-Section Computed Tomography

Class	Radiologic Findings
Type 1	Pure (simple) GGO
Type 2	Semiconsolidation (an area of intermediate homogeneous increase in density)
Type 3	Halo (area consisting of solid part and surrounding GGO halo)
Type 4	Mixed (an area consisting of GGO and solid part having air-bronchogram)
Type 5	Solid pattern with GGO[a]
Type 6	Solid pattern

[a] The area of GGO should be less than 50%.

GGO = ground-glass opacity.

scan. We perform thin-section cuts for every lung tumor 2.0 cm or less in maximal dimension. All tumors were subsequently evaluated with thin-section CT scan. Helical scans with 2-mm collimation were performed through a primary tumor. Images were reconstructed with a high-frequency algorithm, and photographed with a window level of −600 H and a window width of 2,000 H, as a "lung window." Radiologic findings were evaluated by two observers (M.K. and K.S.), who were not informed of the pathologic and prognostic outcome, on thin-section CT scan.

Radiologic Criteria for Grouping

The radiologic findings evaluated were as follows: the maximal tumor dimension, the presence and extent of solid or GGO component in tumor, and homogeneity of tumor. The solid (or consolidation) component was defined as an area of increased opacification more than 5 mm in diameter, which completely obscured underlying vascular markings. Ground-glass opacity was defined as an area of a slight, homogeneous increase in density, which did not obscure underlying vascular markings. Semiconsolidation was defined as an area of an intermediate homogeneous increase in density, which did not obscure underlying vascular markings. A halo was an area that consisted of a solid part and a surrounding GGO halo. Mixed was an area with a heterogeneous increase in density, which consisted of GGO and a solid part with an air-bronchogram. We divided the 373 small adenocarcinomas of the lung into six groups based on the extent of the solid component, presence of GGO, and homogeneity of the tumors (Table 1, Fig 1). Type 1 and 2 tumors are homogeneous in density, and lack a solid component (Figs 2, 3). The density of the tumor distinguishes type 1 from type 2. Type 3 and 4 tumors are heterogeneous in density, and the solid component comprises less than 50% of its diameter. The patterns of the solid component and GGO distinguish type 3 from type 4 (Figs 4, 5). Type 5 and 6 tumors are those that predominantly have a solid component. The presence of GGO distinguishes type 5 from type 6 (Figs 6, 7).

Clinicopathologic Factors and Statistical Consideration

The medical record of each patient was examined for age, sex, histologic tumor type, mode of surgery, serum carcinoembryonic antigen (continuous variable; nanograms per milliliter), pathologic nodal status, lymphatic invasion, vascular invasion, pleural invasion, and intrapulmonary metastasis. Skip metastasis was defined as any mediastinal lymph node involvement by lung cancer without N1 disease. The relationships between these pathologic factors and radiologic classification were investigated in this study to elucidate the prognostic significance of our radiologic classification of peripherally located adenocarcinoma of the lung. To compare two factors, Fisher's exact test was used for statistical analysis. Univariate and multivariate analyses were used to determine which clinical factors predict nodal involvement, such as N1 disease or skip metastasis. Univariate and multivariate analyses were performed by logistic regression analysis using StatView 5.0 (SAS Institute, Inc, Cary, NC). Forward and backward stepwise procedures

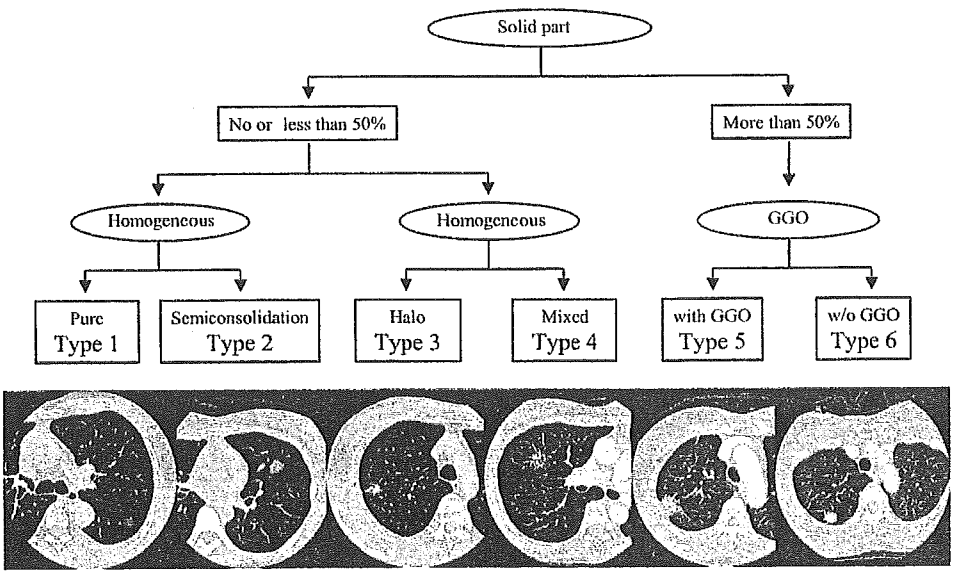

Fig 1. Flow chart for the new classification of small adenocarcinoma of the lung. (GGO = ground-glass opacity; w/o = without.)

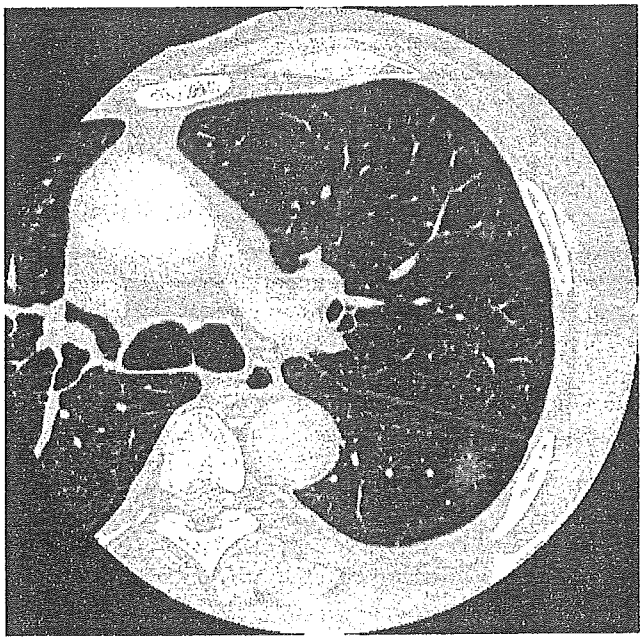

Fig 2. Type 1 tumor is homogeneous in density, and this tumor has been called "pure GGO" or "simple GGO." (GGO = ground-glass opacity.)

were used to determine the combination of factors that were essential in predicting prognosis. Statistical analysis was considered to be significant when the probability value was less than 0.05. Although survival data are shown in this study, this information is considered to be merely suggestive because of the short median follow-up period (just 30 months) for the 341 surviving active patients.

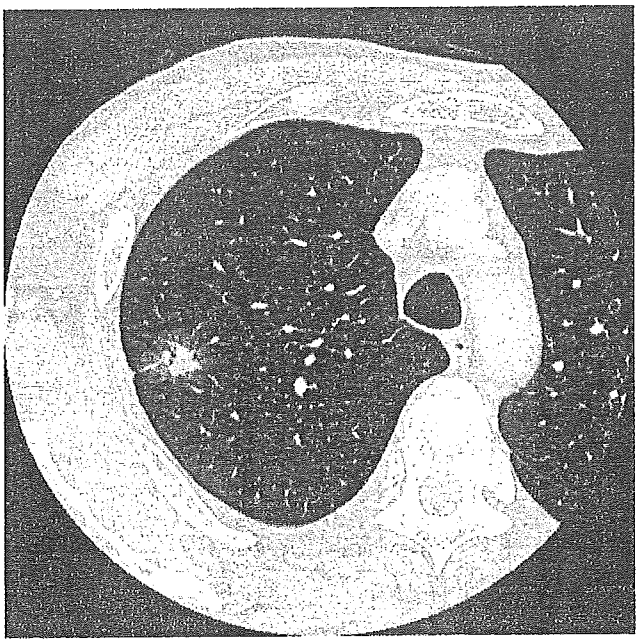

Fig 4. Type 3 tumor is heterogeneous in density, and the solid component comprises less than 50% of its diameter, and is composed of solid and surrounding GGO. (GGO = ground-glass opacity.)

Results

Clinical Characteristics by Radiologic Classifications

Patients with resected adenocarcinoma of the lung 2 cm or less in size were divided into six groups (Table 2). Type 1, 2, 3, 4, 5, and 6 tumors were found in 22 (5.9%), 26 (7.4%), 25 (7.2%), 43 (12.3%), 54 (15.5%), and 179 (51.3%)

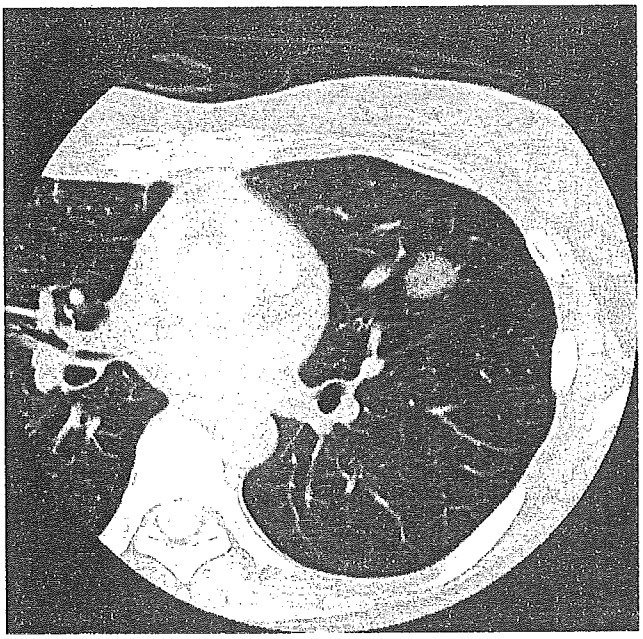

Fig 3. Type 2 tumor is homogeneous in density. It is too dense to call it "pure GGO." The density is much denser than type 1 tumor. (GGO = ground-glass opacity.)

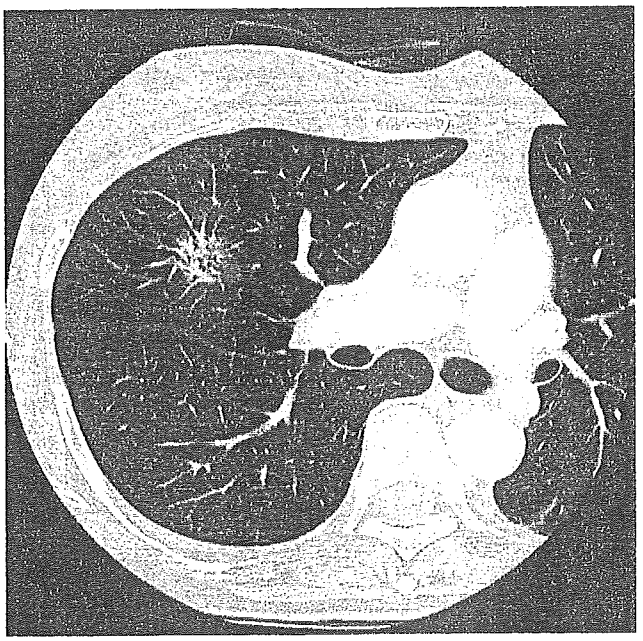

Fig 5. Type 4 tumor is heterogeneous in density, and the patterns of the solid component and GGO distinguish type 3 from type 4. (GGO = ground-glass opacity.)

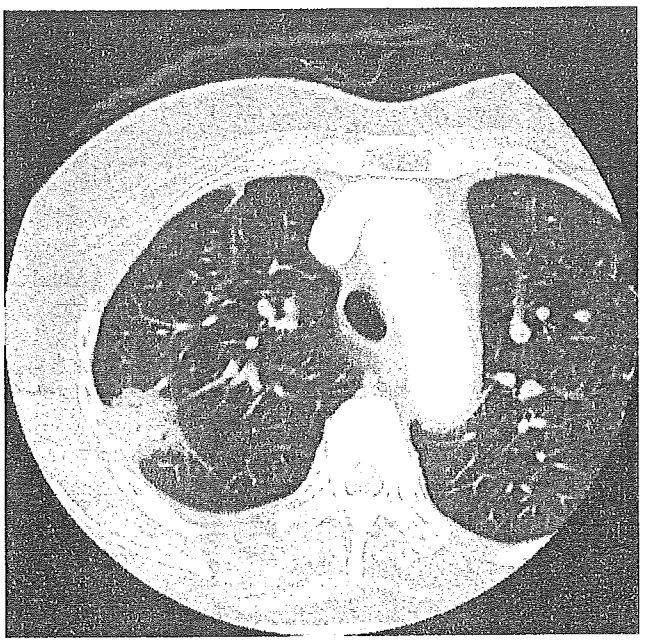

Fig 6. Type 5 tumor predominantly has a solid component and surrounding GGO. (GGO = ground-glass opacity.)

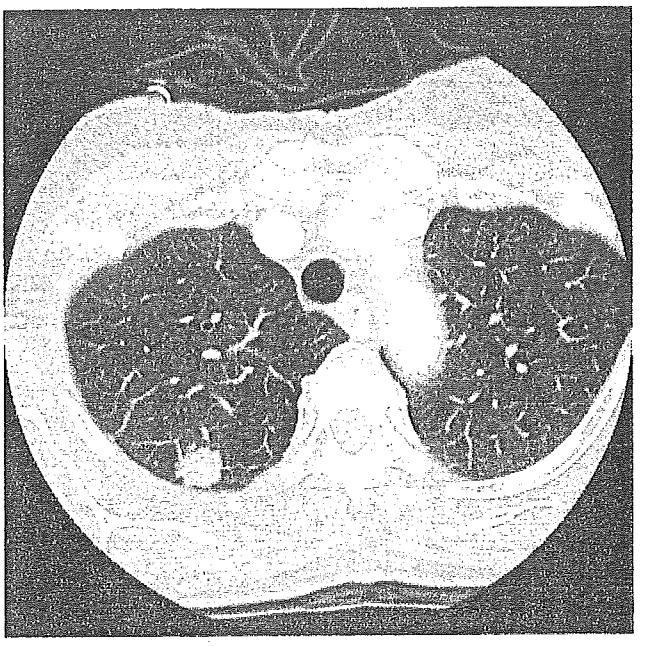

Fig 7. Type 6 tumors predominantly have a solid component. This tumor is so-called pure solid.

patients, respectively. With regard to sex differences, women outnumbered men in each category except type 6. The radiologic maximal tumor dimension ranged from 0.6 to 2.0 cm, with a mean of 1.5 cm, and there were no significant differences among the six categories. Although approximately 20% of patients with type 5 or 6 tumors did not have stage I disease, all but 1 patient with tumors in the other types had stage I disease ($p < 0.001$).

Pathologic Characteristics by the Radiologic Classifications

No nodal involvement was observed among patients with type 1, 2, or 4 tumors. One (4%) patient in type 3 had N1 disease, and 3 patients (5.6%) with type 5 tumors had nodal disease; one N1 and two N2. Type 6 tumors frequently metastasized to regional lymph nodes (43 [24%] patients). Lymphatic invasion was rarely found in patients with type 1, 2, 3, or 4 tumors, whereas this was frequently found in patients with type 5 or 6 tumors ($p < 0.001$). Similar findings were observed for vascular and pleural invasion (Table 3). There were 7 overall deaths, and all died of cancer. All of these patients had lung adenocarcinoma, which showed just a solid component on thin-section CT scan, ie, type 6 tumors. There were no deaths in patients in types 1 to 5, although the median follow-up period for surviving patients is just 30 months.

Table 2. Radiologic Classification and Clinicopathologic Features in Adenocarcinoma of the Lung

Variable	Type 1 Pure GGO	Type 2 SC	Type 3 Halo	Type 4 Mixed	Type 5 Solid & GGO	Type 6 Solid
Number of cases	22 (6.3%)	26 (7.4%)	25 (7.2%)	43 (12.3%)	54 (15.5%)	179 (51.3%)
Mean age (y)	58.6	56.4	64.1	62.3	62.9	62.9
Sex (men/women)	9/13	7/19	11/14	19/24	22/32	99/80
CEA > 5 ng/mL	1	0	1	3	3	40
Radiologic tumor size (cm)						
Range	0.6–1.9	0.8–2.0	0.8–1.9	0.9–2.0	0.9–2.0	0.8–2.0
Mean	1.2	1.4	1.5	1.4	1.5	1.5
Pathologic stage						
IA	21	25	24	43	51	130
IB	1	1	0	0	0	5
IIA	0	0	1	0	0	19
IIB	0	0	0	0	0	4
IIIA	0	0	0	0	2	18
IIIB	0	0	0	0	1	3
IV	0	0	0	0	0	0

CEA = carcinoembryonic antigen; GGO = ground-glass opacity; SC = semiconsolidation.

Table 3. Relationship Between Radiologic Classification and Pathologic Characteristics in Resected Adenocarcinoma of the Lung

Variable	Type 1 Pure GGO	Type 2 SC	Type 3 Halo	Type 4 Mixed	Type 5 Solid & GGO	Type 6 Solid
Total cases	22 (6.3%)	26 (7.4%)	25 (7.2%)	43 (12.3%)	54 (15.5%)	179 (51.3%)
pT1/pT2–T4	21/1	26/0	25/0	43/0	53/1	165/14
Lymph node metastasis	0 (0%)	0 (0%)	1 (4%)	0 (0%)	3 (5.6%)	43 (24%)
pN1/pN2	0/0	0/0	1/0	0/0	1/2	23/20
Skip metastasis	0 (0%)	0 (0%)	0 (0%)	0 (0%)	1 (1.9%)	7 (4.0%)
Lymphatic invasion	1 (5%)	0 (0%)	1 (4%)	0 (0%)	10 (18.5%)	84 (47%)
Vascular invasion	1 (5%)	0 (0%)	0 (0%)	1 (2%)	5 (9.3%)	86 (48%)
Pleural invasion	2 (9%)	0 (0%)	0 (0%)	1 (2%)	4 (7.4%)	48 (27%)

GGO = ground-glass opacity; SC = semiconsolidation.

Clinical Predictors for Nodal Involvement, N1 Disease, and Skip Metastasis

On the basis of multivariate analysis, preoperative carcinoembryonic antigen (nanograms per milliliter; continuous variable) and radiologic findings (types 1 through 4 versus types 5 and 6) were significant predictors for nodal involvement (Table 4). As to N1 disease, preoperative carcinoembryonic antigen (nanograms per milliliter; continuous variable), and radiologic findings (types 1 through 4 versus types 5 and 6) were again significantly associated with pathologic N1 disease (Table 5). None of the clinical factors were detected to be predictors for so-called skip metastasis.

Comment

Recent investigation of small adenocarcinoma of the lung has revealed the pathologic characteristics of these tumors detected by CT scan. Several authors insisted that the prognosis of lung adenocarcinoma with a large area of GGO on thin-section CT scan was much better than that of conventional adenocarcinoma of the lung regardless of the maximal tumor dimension (Table 6) [4, 9–15]. These reports provide interesting material for discussion. If adenocarcinoma with a good prognosis can be diagnosed preoperatively, major lung resection might not be required. Some authors have already adopted segmental resection for small-sized lung cancer, and have reported that it might be acceptable for patients with a tumor of 2.0 cm or less in diameter without nodal involvement [16, 17]. From these reports, a peripherally located lung cancer with no lymph node metastasis is the optimal indication for a more limited anatomic resection. However, it is difficult to determine the pathologic nodal status during surgical resection, and there could be some discrepancy between the results of intraoperative frozen-section diagnosis and the final pathologic diagnosis of lymph node metastasis. Locoregional recurrence has been noted after extended segmental resection, and it is possible that such local recurrence might have been prevented by pulmonary lobectomy. Thus, the preoperative diagnosis of the biologic invasiveness of a lung cancer is crucial whenever surgeons dare to adopt a lesser anatomic resection for a resectable lung cancer, which could raise the question of compromised patients.

According to previous data, lung adenocarcinoma with a large area of GGO shows a good prognosis, and one of the most important prognostic factors is the extent of GGO. However, how can the extent of GGO be evaluated in patients with type 4 adenocarcinoma? Inasmuch as type 4 tumor is made up of a heterogeneous mixture of GGO and a solid part, it is difficult to measure the size of the solid part. As a result, there is considerable disagreement among physicians on the diagnosis. Some may diagnose such tumors as "noninvasive," and others may diagnose them as "invasive" based on CT findings. The reason for this inconsistency is probably that the former radiologic classification is ill-suited for evaluating peripheral lung adenocarcinoma. The extent of GGO is insufficient for the evaluation of all adenocarcinoma of the lung. It may still be difficult for some surgeons to classify small adenocarcinoma of the lung based on our classification.

Among the six types of peripheral small-sized adenocarcinoma, women were predominant in all types except among patients with type 6 tumors. This is an unexpected finding. Traditionally, lung cancer is found more often in men than women. There was no significant difference among the types with regard to the maximal tumor dimension. Regarding small-sized adenocarcinoma of the lung, Noguchi and colleagues [6] investigated prognostic factors based on the findings of central fibrosis. They stated that type A or B tumors should be considered "in-situ" adeno-

Table 4. Results of Multivariate Analysis for Predictors of Nodal Involvement

Variable	Risk Ratio	95% Confidence Interval	*p* Value
CEA (continuous variable; ng/mL)	1.088	1.025–1.155	0.0059
Radiologic classification (type 1–4 vs 5–6)	0.057	0.008–0.427	0.0052

CEA = carcinoembryonic antigen.

Table 5. Results of Multivariate Analysis for Predictors of N1 Disease

Variable	Risk Ratio	95% Confidence Interval	*p* Value
CEA (continuous variable; ng/mL)	1.092	1.029–1.158	0.0037
Radiologic classification (type 1–4 vs 5–6)	0.074	0.010–0.554	0.0112

CEA = carcinoembryonic antigen.

carcinoma of the lung. It is probably safe to say that segmental resection or wide wedge resection is sufficient for such tumors because of their minimally invasive nature. Type 1 tumor is also known as pure GGO or simple GGO [18]. Among 22 type 1 tumors, there was no lymph node metastasis, and pathologic findings showed minimal invasion. There were 15 (68%) tumors that were equivalent to the type A or B tumors of Noguchi and colleagues [6], ie, roughly bronchioloalveolar carcinoma. Type 2 tumor is denser than type 1 tumor on thin-section CT scan. This tumor is not a solid tumor because we can see the underlying bronchovascular structure. No lymph node metastasis was noted, and 11 tumors were similar to the type A or B tumors of Noguchi and colleagues [6]. The difference in their density is probably related to the difference in the amount of air contained in the tumor, ie, differences in alveolar space histologically. Type 3 tumor is also known as GGO halo. One tumor had metastasized to the intrapulmonary lymph node, ie, N1 node, but 15 tumors were still diagnosed as being equivalent to the type A or B tumor of Noguchi and colleagues [6]. Type 4 tumor is actually defined by our original definition. This tumor consists of a mixture of GGO and a solid part containing air, roughly air-bronchogram. There was no lymph node metastasis and no lymphatic invasion. Basically, lung adenocarcinoma in the above four types is thought to be "minimally invasive" adenocarcinoma. A limited anatomic resection of the lung could be the standard surgical procedure for such tumors in the near future.

Type 5 and 6 tumors are considered to exhibit a "solid" course. Lymph node metastasis was found in roughly 5% of type 5 tumors, and 27% of type 6 tumors. Traditionally, lymph node metastasis is found in approximately 15% of small adenocarcinoma 2.0 cm or less in size. According to our results, however, lymph node metastasis was found mostly in type 6, which meant that if peripheral lung adenocarcinoma showed GGO on thin-section CT, the probability of lymph node metastasis was less than 5%. These "solid" tumors could be divided into several subgroups by means of positron emission tomography. If the solid tumors show positive results by positron emission tomography, they may be associated with a high frequency of lymph node metastasis and a poor prognosis.

One of the important objectives of this study is to determine the indication for limited surgical resection for lung adenocarcinomas. From this concept, the classification became simpler if the classification was composed with groups, ie, types 1 through 4 and types 5 and 6. If a tumor belongs to types 1 through 4, the patient would be a candidate for limited surgical resection, whereas a tumor belonging to group 5 or 6 warrants major lung resection with systematic lymph node dissection necessary. However, we believe the six classifications proposed in this study remain important for the surgeon to plan for the management of peripheral lung cancer. For instance, most of the type 1 tumors are bronchioloalveolar carcinoma, and some of them might be indolent tumors. On the contrary, type 2 tumors tend to be adenocarcinoma with invasive foci pathologically and grow in size. Actually we made a plan for a prospective follow-up study for type 1 tumors, not for type 2 tumors. Thus, clinical strategy depends on the six classifications, and we hope to leave the classification intact.

As to the surgical indications for pure GGO tumors, we resected the tumor if it is stable or increased in size. However, from our data, tumors belonging to type 1 could be bronchioloalveolar carcinoma, and are sometimes indolent. Thus, recently we just monitor such type 1 tumors without surgical interventions if the radiologic maximal

Table 6. Review of Literature Regarding Proportion of Ground-Glass Opacity as Radiologic Prognostic Factors in Adenocarcinoma of the Lung

Authors	Year	No.	Cases	Methods	Good Prognosis	Analysis
Jang et al. [9]	1996	14	...	...	Focal area of GGO	Univariate
Aoki et al. [4]	2001	127	Ad, cT1	Dimension	GGO > 0.5	Univariate
Kodama et al. [10]	2001	104	Ad, 2 cm or less	Visual	GGO > 0.5	Multivariate
Takamochi et al. [19]	2001	269	Ad, peripheral	TDR	TDR & CEA	Multivariate
Kim et al. [11]	2001	224	Ad, cT1	Visual	GGO extent	Univariate
Matsuguma et al. [12]	2002	111	Ad, cIA	Visual	GGO > 0.5	Univariate
Takashima et al. [15]	2002	64	Ad, 2 cm or less	CT	GGO > 0.57	Multivariate
Suzuki et al. [14]	2002	69	Ad, cIA	Dimension	GGO > 50%	Univariate
Okada et al. [17]	2003	167	Ad, cT1	TDR	TDR > 0.5	Multivariate
Ohde et al. [13]	2003	98	Ad, cT1	Dimension	GGO > 50%	Univariate

Ad = adenocarcinoma; CEA = carcinoembryonic antigen; cT1 = clinical T1; GGO = ground-glass opacities; TDR = tumor disappearance ratio.

tumor dimension is less than 15 mm. If radiologic findings suggest the tumor as lung cancer, preoperative CT-guided fine-needle biopsies are not always performed because of the high rate of a false-negative result for GGO tumors.

In conclusion, a new radiologic classification of small-sized adenocarcinoma of the lung has been proposed. Because this is the retrospective study, there may be numerous levels of bias. Therefore, we are planning to perform a prospective study of the management of peripheral small adenocarcinoma of the lung. Using the classification, we can easily classify peripheral adenocarcinoma of the lung into six categories, and the classification is significantly associated with pathologic prognostic factors. Future treatment strategies for small-sized adenocarcinoma of the lung may be based on this new radiologic classification.

The authors thank Dr Etsuo Miyaoka, PhD, a professor of Tokyo University of Science, for his technical support for statistical analysis. This work was supported in part by a Grant-in-Aid for Cancer Research from the Ministry of Health and Welfare.

References

1. Auerbach O, Garfinkel L. The changing pattern of lung carcinoma. Cancer 1991;68:1973–7.
2. Travis WD, Travis LB, Devesa SS. Lung cancer. Cancer 1995;75(1 Suppl):191–202.
3. Henschke CI, McCauley DI, Yankelevitz DF, et al. Early Lung Cancer Action Project: overall design and findings from baseline screening. Lancet 1999;354:99–105.
4. Aoki T, Tomoda Y, Watanabe H, et al. Peripheral lung adenocarcinoma: correlation of thin-section CT findings with histologic prognostic factors and survival. Radiology 2001;220:803–9.
5. Shimosato Y, Suzuki A, Hashimoto T, et al. Prognostic implications of fibrotic focus (scar) in small peripheral lung cancers. Am J Surg Pathol 1980;4:365–73.
6. Noguchi M, Morikawa A, Kawasaki M, et al. Small adenocarcinoma of the lung. Histologic characteristics and prognosis. Cancer 1995;75:2844–52.
7. Yokose T, Suzuki K, Nagai K, Nishiwaki Y, Sasaki S, Ochiai A. Favorable and unfavorable morphological prognostic factors in peripheral adenocarcinoma of the lung 3 cm or less in diameter. Lung Cancer 2000;29:179–88.
8. Suzuki K, Yokose T, Yoshida J, et al. Prognostic significance of the size of central fibrosis in peripheral adenocarcinoma of the lung. Ann Thorac Surg 2000;69:893–7.
9. Jang HJ, Lee KS, Kwon OJ, Rhee CH, Shim YM, Han J. Bronchioloalveolar carcinoma: focal area of ground-glass attenuation at thin-section CT as an early sign. Radiology 1996;199:485–8.
10. Kodama K, Higashiyama M, Yokouchi H, et al. Prognostic value of ground-glass opacity found in small lung adenocarcinoma on high-resolution CT scanning. Lung Cancer 2001; 33:17–25.
11. Kim EA, Johkoh T, Lee KS, et al. Quantification of ground-glass opacity on high-resolution CT of small peripheral adenocarcinoma of the lung: pathologic and prognostic implications. AJR Am J Roentgenol 2001;177:1417–22.
12. Matsuguma H, Yokoi K, Anraku M, et al. Proportion of ground-glass opacity on high-resolution computed tomography in clinical T1 N0 M0 adenocarcinoma of the lung: a predictor of lymph node metastasis. J Thorac Cardiovasc Surg 2002;124:278–84.
13. Ohde Y, Nagai K, Yoshida J, et al. The proportion of consolidation to ground-glass opacity on high resolution CT is a good predictor for distinguishing the population of non-invasive peripheral adenocarcinoma. Lung Cancer 2003;42:303–10.
14. Suzuki K, Asamura H, Kusumoto M, Kondo H, Tsuchiya R. "Early" peripheral lung cancer: prognostic significance of ground glass opacity on thin-section computed tomographic scan. Ann Thorac Surg 2002;74:1635–9.
15. Takashima S, Maruyama Y, Hasegawa M, et al. Prognostic significance of high-resolution CT findings in small peripheral adenocarcinoma of the lung: a retrospective study on 64 patients. Lung Cancer 2002;36:289–95.
16. Yoshikawa K, Tsubota N, Kodama K, Ayabe H, Taki T, Mori T. Prospective study of extended segmentectomy for small lung tumors: the final report. Ann Thorac Surg 2002;73: 1055–8.
17. Okada M, Nishio W, Sakamoto T, et al. Effect of tumor size on prognosis in patients with non-small cell lung cancer: the role of segmentectomy as a type of lesser resection. J Thorac Cardiovasc Surg 2005;129:87–93.
18. Mirtcheva RM, Vazquez M, Yankelevitz DF, Henschke CI. Bronchioloalveolar carcinoma and adenocarcinoma with bronchioloalveolar features presenting as ground-glass opacities on CT. Clin Imaging 2002;26:95–100.
19. Takamochi K, Nagai K, Yoshida J, et al. Pathologic N0 status in pulmonary adenocarcinoma is predictable by combining serum carcinoembryonic antigen level and computed tomographic findings. J Thorac Cardiovasc Surg 2001;122:325–30.

INVITED COMMENTARY

Anatomical resection is the standard treatment for early stage nonsmall cell lung cancer. As radiographic scanning methods are improving and we are identifying cancers at smaller sizes than previously recognized, the issue of limited resection for small peripheral cancers is being reinvestigated. Should small size on computed tomography (CT) be the only criteria with which to determine the type of resection (ie, anatomical versus limited [wedge]) to be performed? The answer would be no, according to the article by Suzuki and colleagues [1]. This study is a retrospective review of a single institutional experience in 349 chemotherapy–radiotherapy naive patients with small, single peripheral lung primary adenocarcinomas during a 4-year period of time from 1999 to 2003 to evaluate a new radiographic classification that may assist in the future management of patients. From their classification, in essence a radiologic Noguchi classification [2], they were able to identify a group of patients who might be best treated with limited resection. In their series, the 42 patients with either N1 or N2 disease seemed to have a greater solid component and less ground glass opacification (GGO) features than those who did not have those features. The authors concluded that their classification may be a useful evaluation system for future trials.

Some articles raise more questions than answers, as does this article. Clinicians should not be tempted to follow the authors' implications (given the retrospective design of this study) that thin-section CT peripheral lung

0003-4975/06/$32.00
doi:10.1016/j.athoracsur.2005.09.040

Genetic Classification of Lung Adenocarcinoma Based on Array-Based Comparative Genomic Hybridization Analysis: Its Association with Clinicopathologic Features

Tatsuhiro Shibata,[1] Satomi Uryu,[2] Akiko Kokubu,[1] Fumie Hosoda,[2] Misao Ohki,[2] Tokuki Sakiyama,[3] Yoshihiro Matsuno,[5] Ryosuke Tsuchiya,[6] Yae Kanai,[1] Tadashi Kondo,[4] Issei Imoto,[7,8] Johji Inazawa,[7,8] and Setsuo Hirohashi[1]

Abstract The array-based comparative genomic hybridization using microarrayed bacterial artificial chromosome clones allows high-resolution analysis of genome-wide copy number changes in tumors. To analyze the genetic alterations of primary lung adenocarcinoma in a high-throughput way, we used laser-capture microdissection of cancer cells and array comparative genomic hybridization focusing on 800 chromosomal loci containing cancer-related genes. We identified a large number of chromosomal numerical alterations, including frequent amplifications on *7p12*, *11q13*, *12q14-15*, and *17q21*, and two homozygous deletions on *9p21* and one on *8p23*. Unsupervised hierarchical clustering analysis of multiple alterations revealed three subgroups of lung adenocarcinoma that were characterized by the accumulation of distinct genetic alterations and associated with smoking history and gender. The mutation status of the *epidermal growth factor receptor* (*EGFR*) gene was significantly associated with specific genetic alterations and supervised clustering analysis based on *EGFR* gene mutations elucidated a subgroup including all *EGFR* gene mutated tumors, which showed significantly shorter disease-free survival. Our results suggest that there exist multiple molecular carcinogenesis pathways in lung adenocarcinoma that may associate with smoking habits and gender, and that genetic cancer profiling will reveal previously uncharacterized genetic heterogeneity of cancer and be beneficial in estimating patient prognosis and discovering novel cancer-related genes including therapeutic targets.

Lung cancer is one of the most lethal and increasing cancers in Western countries as well as in Japan (1). Lung cancer is histopathologically divided in two subgroups, small cell lung carcinoma and non-small cell lung carcinoma, and lung adenocarcinoma comprises >40% of the latter (1).

Previous genetic analyses using allelotyping, comparative genomic hybridization (CGH), or the candidate gene approach revealed many genomic (genetic and epigenetic) alterations of tumor suppressor genes (such as *p53*, *p16^{INK4a}*, *FHIT*, *LKB1*, and *PTEN*) and oncogenes [such as *K-ras*, *B-RAF*, *MYC*, *epidermal growth factor receptor* (*EGFR*), and *ERBB2*] as well as many chromosomal imbalances (such as on 3p, 8p, 9p, 17p, 18q, and 19p) in lung adenocarcinomas (2-10). However, overall understanding of genomic alterations in lung adenocarcinomas is far from complete and analysis of the relationship between the overall profile and combinations of genetic alterations with clinicopathologic parameters is still lacking. Recently, genome-wide gene expression analyses have uncovered a novel dimension of cancer profiling and helped define the nature of the heterogeneous subgroups of lung adenocarcinoma, each of which shows distinct tumor histology and patient prognosis (11-14). However, it is unclear whether there exist multiple genomic pathways in lung adenocarcinoma because of the lack of a genome-wide view of genetic alterations. It is clinically important to examine the correlations of certain molecular-genetic pathways with cancer cell traits relating to patient prognosis or chemotherapy sensitivity because it is possible that genetic alteration profiling may predict tumor recurrence/metastasis or sensitivity to molecular-target therapies as well as mRNA or protein expression profiles do (15-17).

The recently developed array-based CGH method using microarrayed bacterial artificial chromosome clones allows high-resolution analysis of genome-wide copy number changes in various tumors (18, 19). To define and analyze the genetic alterations of lung adenocarcinoma in a more detailed way,

Authors' Affiliations: [1]Pathology Division, [2]Cancer Genomics Project, [3]Center for Medical Genetics, [4]Cancer Proteomics Project, National Cancer Center Research Institute, Tokyo, Japan; [5]Clinical Laboratory and [6]Thoracic Surgery Divisions, National Cancer Center Hospital, Tokyo, Japan; [7]Department of Molecular Cytogenetics, Medical Research Institute, Tokyo Medical and Dental University, Tokyo, Japan; and [8]Core Research for Evolutional Science and Technology of Japan, Science and Technology Corporation, Saitama, Japan

Received 2/8/05; revised 5/31/05; accepted 6/17/05.

Grant support: Grant-in-Aid for the Comprehensive 10-Year Strategy for Cancer Control from the Ministry of Health, Labor and Welfare, Japan.

The costs of publication of this article were defrayed in part by the payment of page charges. This article must therefore be hereby marked *advertisement* in accordance with 18 U.S.C. Section 1734 solely to indicate this fact.

Requests for reprints: Setsuo Hirohashi, Pathology Division, National Cancer Center Research Institute, 5-1-1, Tsukiji, Chuo-ku, 104-0045 Tokyo, Japan. Phone: 81-3-3547-5201, ext. 4101; Fax: 81-3-3248-2463; E-mail: shirohas@ncc.go.jp.

doi:10.1158/1078-0432.CCR-05-0293

we used the array CGH technique and laser-capture microdissection of cancer cells, a combination that we have successfully used in other tumor types (20).[9] Using these two powerful methodologies enabled us to detect a considerable number of novel chromosomal numerical alterations in primary lung adenocarcinoma. Unsupervised and supervised hierarchical clustering analyses of genome-wide genetic alterations revealed the presence of heterogeneous groups of lung adenocarcinoma, which are characterized by specific combinations of genetic alterations, varying *EGFR* gene mutation status, and tumor recurrence rates.

Materials and Methods

Patient materials. Surgical specimens of 55 lung adenocarcinoma patients who had been diagnosed and undergone operation between June 2001 and May 2002 at the National Cancer Center Hospital were examined. Fragments of tumor and corresponding normal lung tissue were taken immediately after surgery, fixed with 100% methanol, and embedded in paraffin. This study was approved by the institutional review boards of the National Cancer Center. The clinicopathologic data of the patients are shown in Table 1.

Laser-capture microdissection and whole-genome amplification. Laser-capture microdissection was done using LM200 (Arcuturus, Mount View, CA) as described (21). Only cancer cells were microdissected and lymphocytes, fibroblasts, and endothelial cells were carefully excluded. Corresponding normal lung epithelial cells were similarly microdissected and used as reference. To amplify the genomic DNA fragments, we used an adaptor-ligated whole-genome PCR as previously reported (22).

Array-based comparative genomic hybridization. This study used a custom-made CGH array called "MCG CancerArray-800 ver.2," which consists of 800 duplicated bacterial artificial chromosome clones corresponding to various chromosomal loci that have been reported or considered to be altered in various human cancers (20, 23). Details of hybridization procedures have been previously reported (20). Sixteen-bit fluorescence intensity TIF images were obtained using a scanner (FLA8000, Fuji Film, Tokyo, Japan) and analyzed using GenePix Pro 5.0 (Axon Instruments, Inc., Foster City, CA). Thresholds for chromosomal gain (ratio >1.25) and loss (ratio <0.75) were determined by "normal versus normal experiments" (23, 24). We also validated our array CGH data by other methods. Loss of the *17p13* locus was confirmed by loss of heterozygosity of the *p53* gene, which is located within that bacterial artificial chromosome using a microsatellite marker (TP53CA). Gene amplification of a representative gene, *cyclin D1*, was validated by fluorescence *in situ* hybridization analysis (24). We applied multiplex ligation-dependent probe amplification (MLPA) to validate ourarray data. Copy number alterations of multiple loci were analyzed using MLPA-SALSA kit (MRC-Holland, Amsterdam, the Netherlands) as per the recommendation of the manufacturer (25). Size and quantity of PCR products were calculated by Gene Mapper software (Version 3.5, Applied Biosystems, Tokyo, Japan) and copy number was determined by the ratio to the average of five normal control experiments.

Mutational analysis. We amplified exons 18, 19, 21, and 23 of the *EGFR* gene; exons 2 and 3 (covering codons 12, 13, and 61) of the K-*ras* gene; exons 20 and 21 of the *ERBB2* gene; and exons 10, 14, 16, 17, 18, 19, and 20 of the *MET* gene from microdissected tumor and corresponding normal DNA samples with PCR using High Fidelity Taq polymerase (Roche, Mannheim, Germany) and appropriate primers (primer sequences are available on request). All PCR products were purified and analyzed by sequencing. PCR products showing deletions were subcloned in TA-vector (Invitrogen, Carlsbad, CA) and sequenced.

[9] Unpublished data. Shibata T, Hosoda F, Ohki M, Hirohashi S.

Table 1. The clinicopathologic characteristics and oncogenic mutation profiles of patients and tumors

	No. cases	Frequency (%)
Total no. patient	55	
Mean age (range)	62.3 (35-79)	
Gender		
Male	28	50.9
Female	27	49.1
Smoking history		
Never	27	49.1
Former	10	18.2
Current	18	32.7
Tumor differentiation		
Well	20	36.4
Moderate	25	45.5
Poor	10	18.1
Stage*		
I (IA and IB)	24	43.6
II (IIA and IIB)	6	10.9
III (IIIA and IIIB)	21	38.2
EGFR mutation	26	47
Exon 18 G719S	1	1.8
Exon 19 Del746-750	8	14.5
Exon 19 Del747-752	2	3.6
Exon 19 Del747-752insS	1	1.8
Exon 21 L858R	14	25.5
K-*ras* mutation	6	11
Codon 12	4	7.3
Codon 13	1	1.8
Codon 61	1	1.8

*Clinical stage of four cases was not evaluated.

Immunohistochemical analysis. Four-micrometer sections of formalin-fixed, paraffin-embedded specimens of lung adenocarcinoma were stained with an anti-MET mouse monoclonal antibody (×100 dilution, Zymed, San Francicso, CA) as the suppliers recommended.

Statistical analysis. Two-dimensional hierarchical clustering analysis of the samples and signal ratios was done using the Impressionist (Gene Data, Basel, Switzerland) and GeneMaths (Applied Maths, Sint-Martens-Latem, Belgium) software programs as described (26, 27). Data were standardized by dividing by the root means and dendrograms were produced using the Pearson Correlation algorithm. For supervised clustering, we first selected loci that were significantly different between *EGFR* wild-type and mutated tumors based on the average ratio by Student's *t* test. We then used a machine-learning method, in which the leave-one-out cross-validation was done with all combinations of loci and multiple independent classifier algorithms, and selected 46 loci that could discriminate *EGFR* mutation status most accurately to classify the tumors. The Kaplan-Meier method was used to estimate the probability of disease-free survival. Cox proportional hazards regression model and multivariate analysis were done to detect the association between the presence of chromosomal alterations and disease-free survival. Log-rank analysis was used to assess the significance of the difference between subgroups.

Results

Array-based comparative genomic hybridization analysis of primary lung adenocarcinoma. We analyzed 55 cases of lung

adenocarcinoma by array-based CGH and the chromosomal alteration profiles of 800 loci are shown in Fig. 1. We identified 32 loci that were lost in >40% of cases (Table 2). Among them, the *9p21* locus containing the $p16^{INK4a}$ gene and the *17p13.1* locus containing the *p53* gene were lost in 54% and 40% of analyzed cases, respectively. We found homozygous deletions of three loci, including two on *9p21* and one on *8p23.3*. We also identified 19 loci that were gained in >50% of cases (Table 3) and recurrent (>4 cases) amplifications (>4 copies) on *12q14-15* (9 of 55, 16.3%) followed by *7p12.3* (5 of 55), *11q13* (5 of 55), *17q12* (5 of 55), *1p36.1* (4 of 55), *1q21* (4 of 55), *5p15* (4 of 55), *7q31* (4 of 55), *8q24* (4 of 55), *14q12* (4 of 55), and *17q21.2* (4 of 55). These included genes previously reported to be amplified in lung cancer, such as the *cyclin D1* (*11q13*), *EGFR* (*7p12.3*), and *ERBB2* (*17q21.2*) genes (28, 29). We further validated copy number alterations on *8q24.3*, *17q21.2*, *3p21*, and *17p13.1* by MLPA method. Chromosomal copy number changes (both gains and losses) detected by array CGH corresponded to those by MLPA (Fig. 1C).

Unsupervised hierarchical clustering of array comparative genomic hybridization data. To examine whether there exist multiple carcinogenesis pathways in lung adenocarcinoma, we attempted two-dimensional hierarchical profiling of the chromosomal alterations detected. We first plotted the number of loci showing various incidences of alterations and found that there exist two peaks (loci altered in 10-15% and 20-25% of cases; Fig. 1D). We assumed that alterations appearing in <20% of cases reflect mostly random alterations as observed in genome-wide allelotyping analyses (30), whereas alterations affecting >20% of cases probably represent nonrandom (cancer-specific) alterations. Therefore, to exclude random changes that may be caused by the intrinsic genetic instability of cancer, we selected the loci that were affected in >25% of analyzed cases (397 loci in total) and did the unsupervised hierarchical clustering analysis. When analyzed by using loci affected in >5% and 15% of cases, we obtained almost the same classification as described below (data not shown).

Our hierarchical clustering yielded three distinct subclasses of primary lung adenocarcinoma (clusters A, B, and C shown in Fig. 1E). Cluster B exhibited significantly fewer genetic alterations (losses and gains) in all examined clones than the other two clusters; the average number of alterations (losses, gains, total) in cluster A was 102, 141, and 244, respectively; in B 43, 81, and 125; and in C 85, 131, and 216 (A versus B: $P < 0.0001$; B versus C: $P < 0.0001$). Frequencies of the various lost or gained loci were significantly different among these three cluster groups ($P < 0.01$). Cluster A was characterized by gains on *1p32-26*, *4p16.3*, *11p15*, *12q13-14*, *16p11.2-13.3*, *17q11.1-25*, *19q13.2*, *20p11*, *20q11.2*, and *22q12.2* and losses on *1p22*, *6q26*, *10q24-26*, *13q22.1-34*, *15q21-25*, and *18p11.2*. Cluster C significantly showed gains on *5p12-14.3*, *7p12.3-21.1*, *7q22*, *7q31*, *8q12-21*, and *14q11-24*, and losses on *1q23.3-41*, *10q22.1*, and *Xq*. Some loci were similarly altered in both clusters A and C, including losses on *3p21-24*, *6q26*, *8q24.3*, *9q21*, *10p15*, *10q11*, *10q26*, *15q21.1*, *15q26.1*, and *19p13.3* (containing *LKB1*), and gains on *5p15*, *6p21*, *7p21-22*, *7q21*, *8q21*, *8q22-24* (containing *MYC*), *9q21-22*, *11q13* (containing *cyclin D1*), and *20q13.1*. Losses on *3p14* (containing *FHIT*), *8p22-23.3*, *9p21* (containing $p16^{INK4a}$), *13q11-34*, *17p13.1* (containing *p53*), *18q21*, and gains on *1q21-23*, *1q42*, *7p15*, *17q12*, *17q21.2*, and *17q25* were observed in all subgroups with similar frequency. Two alterations (a gain on *19q13.1* and a loss on *22q12.2*) were more frequently observed in cluster B than in clusters A and C. The above classification into cluster groups showed significant correlation with the patients' smoking history ($P < 0.01$) and gender ($P < 0.001$); cluster A frequently contained female patients without any smoking history (female: 17 of 20 cases and never smoker: 14 of 20 cases), whereas cluster B included male patients with current or former smoking history (male: 11 of 15 cases and smoker: 11 of 15 cases). Cluster C included more male patients (male: 14 of 20 cases), but showed no significant association with smoking history (smoker: 11 of 20 cases). No significant differences were observed between the groups with regard to other clinical features (histologic differentiation, clinical stage, and disease-free survival). Multivariate analysis revealed that two chromosomal alterations showed significant association with disease-free survival: a loss on 13q14.1 ($P = 0.01$, hazard ratio, 3.21; 95% confidence interval, 1.30-7.91) and a gain on 8q24.2 ($P = 0.02$, hazard ratio, 2.92; 95% confidence interval, 1.16-7.37).

It has been reported that somatic mutations of the K-*ras*, *EGFR*, and *ERBB2* genes are frequent in lung adenocarcinoma (2, 8-10, 31-33). We attempted to determine the correlation of these oncogenic mutations with the above classification. We sequenced exons covering the kinase domain of the *EGFR* gene and found somatic mutations in 26 cases (47%; Table 1). *EGFR* mutations were more frequently observed in never-smoker patients ($P < 0.001$) and in the A and C cluster groups ($P = 0.01$ and 0.02). We detected K-*ras* activating mutations in six cases (11%; Table 1) and *EGFR* and K-*ras* mutations were mutually exclusive in our cases as reported by others (31, 32). No mutation in the reported exons of the *ERBB2* gene was detected.

Supervised clustering analysis revealed correlation of EGFR gene mutation with specific genetic alterations. Tumors with *EGFR* mutations showed significantly more genetic alterations (losses and gains) than those without *EGFR* mutations; the average numbers of alterations (losses, gains, total) were 68, 110, and 178 in *EGFR* wild-type tumors and 93, 134, and 227 in *EGFR* mutated tumors, respectively (wild-type versus mutated $P = 0.01$, 0.03, and 0.01). We found 58 loci that showed significant differences in the frequency of copy number alterations between *EGFR* wild-type and mutated tumors. To further examine the genetic profile of *EGFR* mutated tumors, we classified lung adenocarcinomas based on their *EGFR* mutation status with the use of supervised hierarchical clustering. We preformed a machine-learning method with leave-one-out cross-validation and selected 46 loci that could discriminate *EGFR* mutation status. *EGFR* wild-type and mutated tumors were clustered in distinct groups using the ratios of 46 selected loci (Fig. 2A). Tumors carrying K-*ras* mutations were segregated from the *EGFR* mutant branch (Fig. 2A). Interestingly, some cases without *EGFR* mutation were clustered with the mutant branch, and tumors carrying *EGFR* mutations were separated in two subbranches (EGFR-MUT-A and EGFR-MUT-B; Fig. 2A). One branch (EGFR-MUT-A) was characterized by amplification of *12q14* or *1p36.1*, whereas the other (EGFR-MUT-B) contained frequent amplification of *7p12.3* (containing the *EGFR* gene), *1q44-23*, *5p12*, *14q31*, and *16p13.3*. Poorly differentiated tumors were significantly ($P = 0.01$) segregated in the EGFR-MUT-B subgroup (EGFR-MUT-A: 1 of 15 cases and EGFR-MUT-B: 5 of 21 cases).

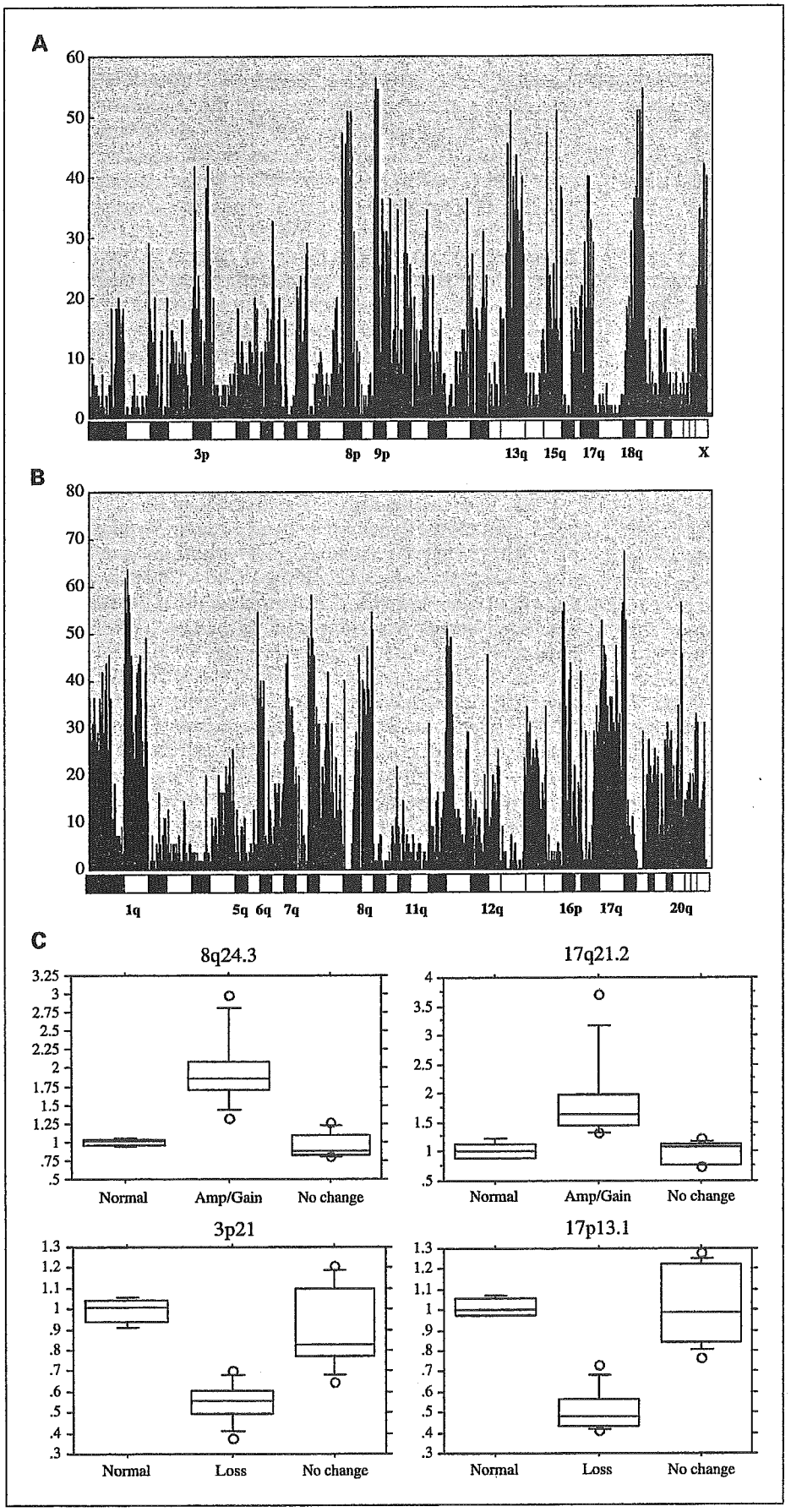

Fig. 1. Copy number alteration profiles of primary lung adenocarcinoma. Frequencies (%) of chromosomal losses (*A*) and gains (*B*) detected by array CGH analyses are plotted from chromosome 1p (*left*) to Y (*right*). Each chromosome is represented by underlining boxes (short and long arms are indicated by closed and open boxes, respectively). Chromosomal arms that contain frequent losses or gains are also indicated. *C*, validation of array CGH analysis. Distributions of copy number on *8q24.3, 17q21.2, 3p21*, and *17p13.1* loci detected by MLPA method in five normal samples (*Normal*), tumors with alterations detected by array CGH (*Amp/Gain* or *Loss*), and tumors without alteration by array CGH method (*No change*) were shown.

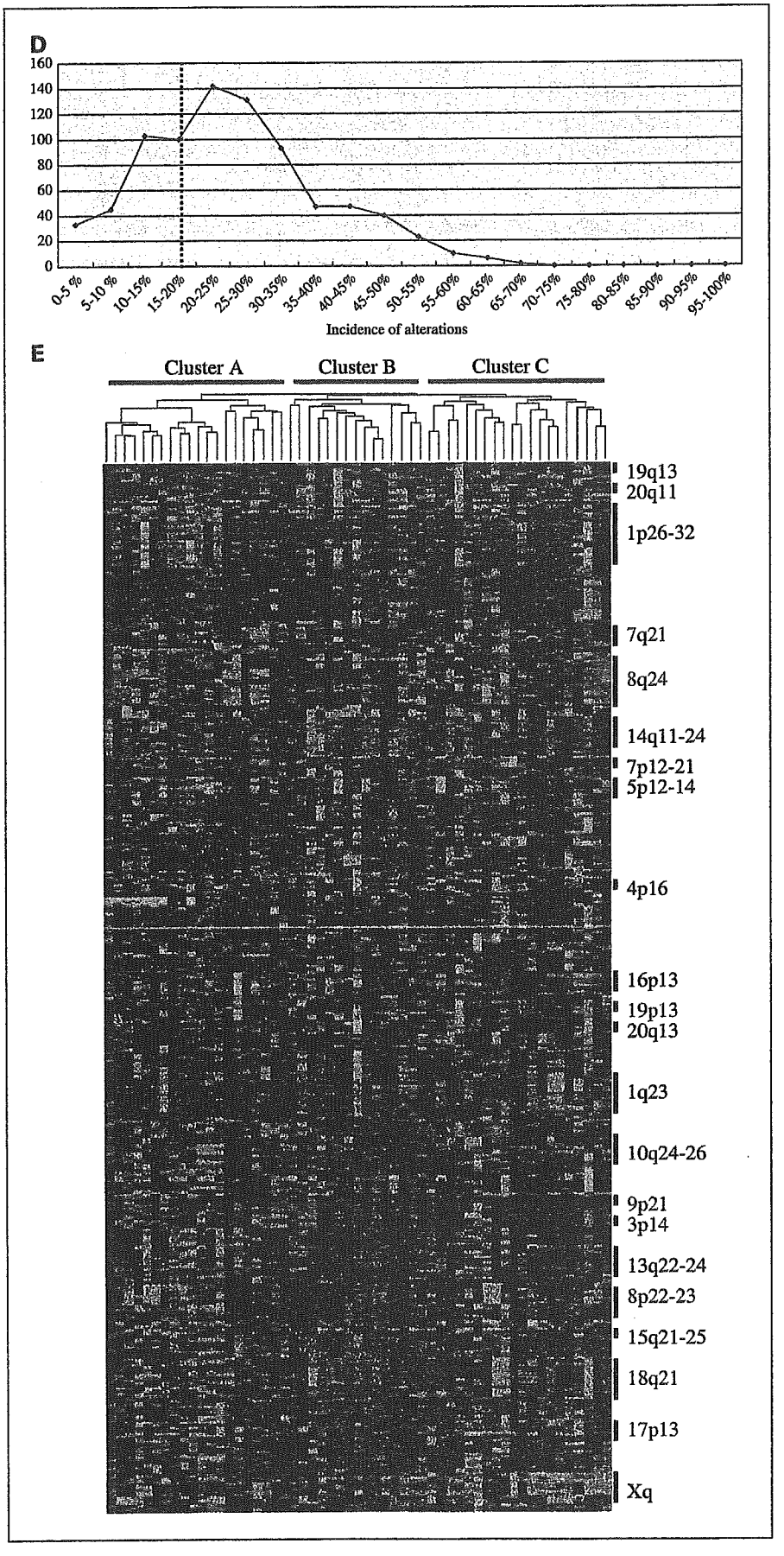

Fig. 1. *Continued.* *D* and *E*, genetic classification of lung adenocarcinoma. *D*, number of loci as a function of the percentage of altered loci in lung adenocarcinoma. Two modes, which can be separated by the vertical dotted line, can be observed. Loci within the first mode (altered in <20% of cases) were considered random, whereas those in the second mode (altered in >20% of cases) were considered pathogenic. *E*, unsupervised genetic profiling of lung adenocarcinoma. Fifty-five lung adenocarcinomas were clustered hierarchically on the basis of copy number changes in 397 loci. Multiple lost (*green*) or gained (*red*) loci are observed in individual tumors. Overall pattern of standardized gene copy numbers and the cluster tree of individual tumors are shown. Tumors were clustered in three subgroups (clusters A, B, and C). Loci that are specific for (*black letters*) or shared with (*blue letters*) each subgroup are indicated on the right side.

The *EGFR* wild-type tumors that were clustered with the EGFR-MUT branch led us to hypothesize that aberrant activation of tyrosine kinases other than *EGFR* have an effect equivalent to that of *EGFR* mutations in these tumors. We examined the copy number changes of loci containing oncogenic receptor-type tyrosine kinases (FGFR1, FGFR2, FGFR3, PDGFR, KIT, MET, ERBB2, FLT3, NTRK1, and NTRK3) detected by our arrays. We found that amplification of a locus containing the *MET* gene (*7q31*) was observed in *EGFR* wild-type tumors (three of four amplified cases; a representative case was shown in Fig. 3A) and that these tumors were clustered with the EGFR-MUT branch (Fig. 2A). Overexpression of MET protein was immunohistochemically detected in 24% (13 of 55) of cases including all cases with amplification of the *MET* gene (Fig. 3B), although there was no significant association between MET overexpression and the clustering. To determine whether somatic mutations of this kinase also occur in lung adenocarcinoma, we sequenced the exons of the *MET* gene, which have been reported to exhibit activating mutations in various tumors (34–36); however, no mutation was found in any of examined 55 cases.

We further examined whether this classification is of clinical significance. Kaplan-Meier plots showed a statistically significant difference in disease-free survival between the two groups (EGFR-WT and EGFR-MUT; log-rank analysis, $P = 0.01$; Fig. 2B) although *EGFR* mutation status alone did not (log-rank analysis, $P = 0.06$; data not shown).

Table 2. Loci frequently lost in primary lung adenocarcinoma

Chromosomal location	Covered candidate gene	Chromosomal loss in lung adenocarcinoma (%)
9p22	*MLLT3*	56.4
9p21	*p16^{INK4a}* *	54.5
9p21	*TEK*	54.5
18q23d	*CTDP1*	54.5
9p23	*GASC1*	52.7
9p21.3	*MTAP*	52.7
15q25	*NTRK3*	50.9
13q14.1	*FKHR*	50.9
18q21	*SMAD4**	50.9
8p22	*NAT2*	50.9
18q21.3	*PI5*	50.9
18q21	*GRP*	50.9
18q22	*BCL2*	50.9
8p22	*LZTS1**	49.1
15q12	*SNRPN*	47.3
8p23.3	*D8S504*	47.3
18q21.3	*SCCA1*	47.3
8p22	*N33*†	45.5
13q11-12	*FGF9*	45.5
8p22-11	*NRG1*	43.6
13q22.1	*KLF12*	43.6
Xq28	*MAGEA2*	41.8
3p24.3	*THRB**	41.8
3p14.2	*FHIT**	41.8
8p22-21.3	*DLC1*†	41.8
8p23.1	*AAC1*	41.8
17p11.2	*RH68621*	40
13q14.1	*LCP1*	40
8p22-8p21	*TNFRSF10B*	40
13q33	*EFNB2*	40
17p13.1	*RCV1*	40
18q21.3	*FVT1*	40

*Loss of heterozygosity or mutations, and †aberrant expression was previously reported in lung cancer (3–5).

Table 3. Loci frequently gained in primary lung adenocarcinoma

Chromosomal location	Covered candidate gene	Chromosomal gain in lung adenocarcinoma (%)
17q25	*MAFG*	67.3
1q21	*MUC1**	63.6
1q21	*MCL1**	61.8
7p21	*IL6*	58.2
1q21	*ARHGEF2*	58.2
16p13.3	*ABCA3*	56.4
17q11	*ITGB4*	56.4
20q13	*Livin-2*	56.4
5p15	*TERT*	54.5
8q24	*GLI4*	54.5
16p13.3	IGFALS	54.5
17q24-25	*GRB2*	54.5
1q21	*AF1Q*	54.5
1q23.1	*PMF1*	54.5
12q24	*stSG8935*	52.7
17q12	*PPARBP*	52.7
17q25	*Survivin**	50.9
8q24	RECQL4	50.9
11q12-13	RELA	50.9

*Aberrant expression was previously reported in lung cancer (3–5).

Discussion

This study is the first high-resolution copy number analyses of primary lung adenocarcinoma by array CGH method. To extract common and specific genetic alterations, we collected and analyzed 55 cases of primary lung adenocarcinoma by combining the array-based CGH analysis with laser-capture microdissection of tumor cells. Importantly, our results were validated by the elucidation of frequent alterations of previously reported cancer-related genes in lung adenocarcinoma, including losses on the *p16^{INK4a}*, *p53*, and *FHIT* loci, and amplifications on the *cyclin D1* and *EGFR* loci. Moreover, we elucidated novel frequent alterations in small chromosomal regions such as losses on *13q11-14* and *15q12-25* and gains on *17q25*, *1q21*, and *16p13.3*, which have not been detected by previous studies. Novel recurrent amplification, which may be a landmark for the existence of oncogenes, was also detected on loci, including *1p36.1*, *1q21*, *5p15*, *12q14-15*, and *14q12*. We also found a homozygous deletion on *8p23.3* accompanied with frequent chromosomal loss and identification of candidate tumor suppressor genes in this locus is in progress.

It has been argued that there are distinct subclasses of lung adenocarcinoma by histopathologic observations and recent gene expression profilings (2, 13). Girard et al. (30) reported the possibility of classification of lung cancer by genome-wide allelotyping although their study only examined lung cancer cell lines and could not discriminate between copy number gain and loss. In our study, we analyzed primary lung adenocarcinoma and used unsupervised hierarchical cluster analysis to identify three groups of lung adenocarcinoma based on their distinct genetic changes. Among them, two subclasses (clusters A and C, 20 of

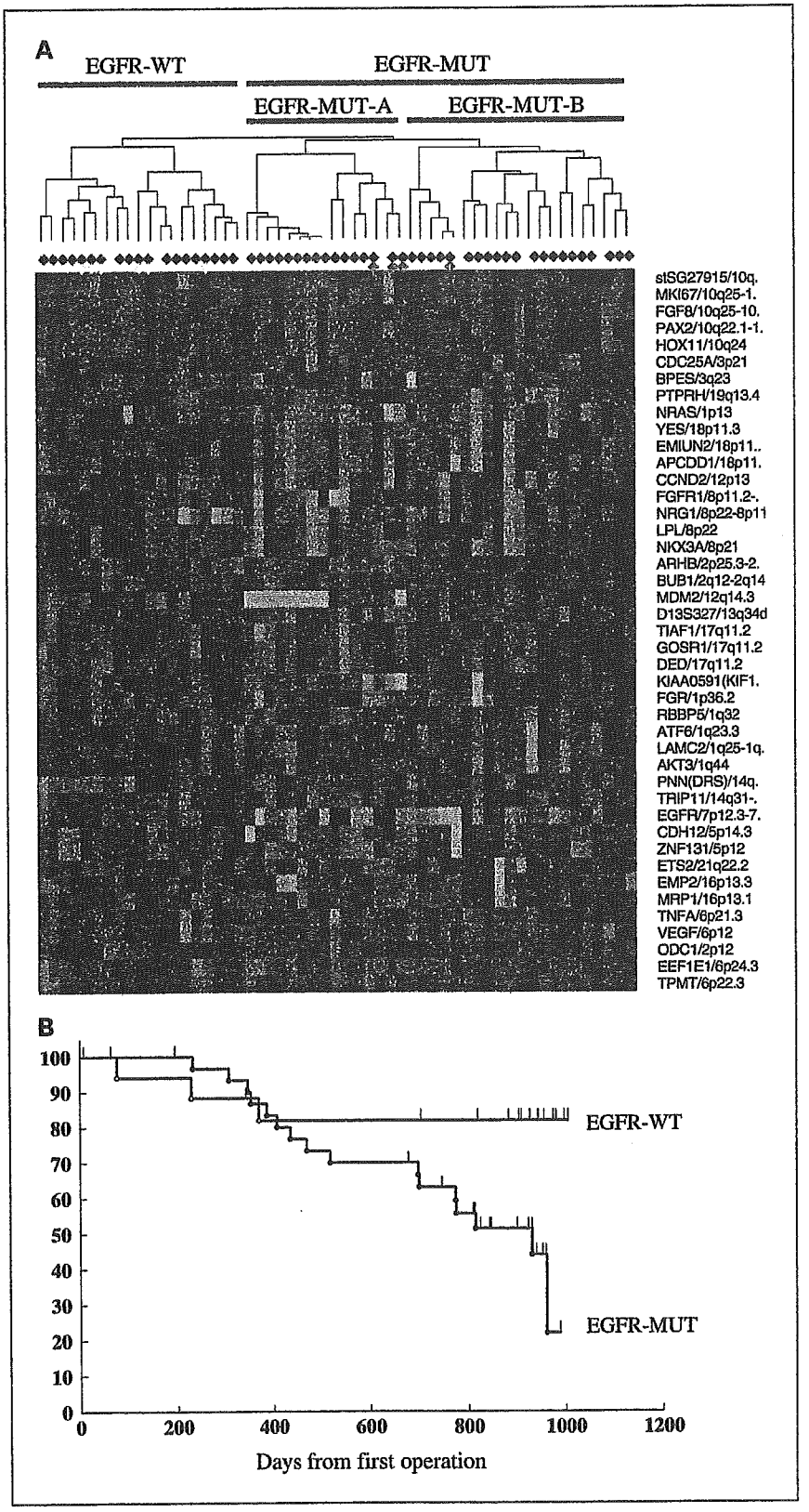

Fig. 2. Supervised genetic profiling of *EGFR* mutation – related loci. *A*, Hierarchical clustering determined copy number change patterns against 46 loci that were identified using the training testing, cross-validation analysis. Lost (*green*) or gained (*red*) loci were indicated in individual tumors. Tumors are classified into two branches (EGFR-WT and EGFR-MUT). All *EGFR* mutated tumors (*red spot*) are clustered in the EGFR-MUT branch. Most tumors without *EGFR* mutations (*blue spot*) are clustered with the EGFR-WT branch, although some are clustered with the EGFR-MUT branch. Six tumors carrying K-*ras* mutations (*yellow spot*) are clustered with the EGFR-WT branch and four MET-amplified tumors (*green spot*) are clustered with the EGFR-MUT branch. The EGFR-MUT branch is subdivided into two subgroups (EGFR-MUT-A and EGFR-MUT-B) with distinctive genetic changes. *B*, genetic profiles and patient disease-free survival. Relationship between patients' disease-free survival and genetic classification based on the *EGFR* mutation – related loci. EGFR-WT and EGFR-MUT groups were significantly different ($P = 0.01$).